Cosmic ray signatures of a 2–3 Myr old local supernova

M. Kachelrieß,[1] A. Neronov,[2] and D. V. Semikoz[3,4]
[1]*Institutt for fysikk, NTNU, N-7491 Trondheim, Norway*
[2]*Astronomy Department, University of Geneva, Chemin d'Ecogia 16, Versoix 1290, Switzerland*
[3]*APC, Universite Paris Diderot, CNRS/IN2P3, CEA/IRFU, Observatoire de Paris, Sorbonne Paris Cite, 119 75205 Paris, France*
[4]*National Research Nuclear University MEPHI (Moscow Engineering Physics Institute), Kashirskoe Highway 31, 115409 Moscow, Russia*

(Received 13 October 2017; published 20 March 2018)

The supernova explosion which deposited ^{60}Fe isotopes on Earth 2–3 million years ago should have also produced cosmic rays which contribute to the locally observed cosmic ray flux. We show that the contribution of this "local source" causes the "anomalies" observed in the positron and antiproton fluxes and explains why their spectral shapes agree with that of the proton flux. At the same time, this local source component accounts for the difference in the slopes of the spectra of cosmic ray nuclei as the result of the slightly varying relative importance of the "local" and the average component for distinct CR nuclei. Such a "local supernova" model for the spectra of nuclei can be tested via a combined measurement of the energy dependence of the boron-to-carbon (primary-to-secondary cosmic rays) ratio and of the antiproton spectrum: while the antiproton spectrum is predicted to extend approximately as a power law into the TeV range without any softening break, the B/C ratio is expected to show a "plateau" at a level fixed by the observed positron excess in the 30–300 GeV range. We discuss the observability of such a plateau with dedicated experiments for the measurement of the cosmic ray composition in the 10 TeV energy range (NUCLEON, ISS-CREAM).

DOI: 10.1103/PhysRevD.97.063011

I. INTRODUCTION

The spectra of cosmic rays (CR) measured locally possess a number of puzzling features which are not well explained assuming a smooth distribution of CR sources, as it is often done in the conventional diffusion approach [1]. In particular:

(i) the slopes of the spectra $dN/d\mathcal{R}$ of different nuclei slightly differ [2–4], although both acceleration and diffusion depend only on rigidity $\mathcal{R} = cp/Z$;
(ii) the spectra of different nuclei show a softening above $\simeq$10 GV, followed by a hardening above several hundred GV [2–7];
(iii) the spectrum of positrons shows an excess above the energy $E \simeq 30$ GeV compared to the naive expectation from secondary production during propagation of CR nuclei in the interstellar medium [8,9];
(iv) similarly, the spectrum of antiprotons above $\simeq$100 GeV is harder than expected from secondary production [10,11];
(v) the positron and antiproton fluxes above 100 GeV repeat the spectral shape of the proton flux; in contrast, the electron flux is considerably steeper [9,11], as shown in Fig. 1;
(vi) the amplitude δ of the dipole anisotropy of the CR flux has a nearly constant level in the 1–30 TV rigidity range, contrary to the expected increase $\delta \propto D(\mathcal{R})$ proportional to the rigidity dependence of the diffusion coefficient $D(\mathcal{R})$ [12].

A "patchwork" of different solutions has been suggested to explain subsets of the features (i)–(vi). Additional sources of primary positrons such as pulsars [13], or annihilations or decays of dark matter [14] may explain the observed

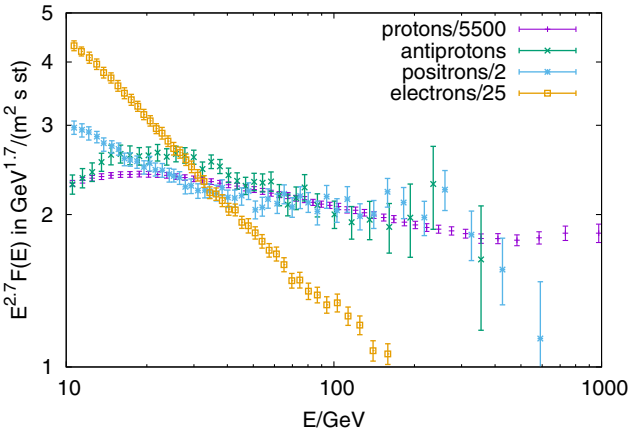

FIG. 1. Proton flux (rescaled by 1/5500), electron flux (rescaled by 1/25), positron flux (rescaled by 1/2), and the antiproton flux measured by AMS-02; all multiplied by $E^{2.7}$.

positron excess (iii). Uncertainties of the antiproton production cross section and of CR propagation models are invoked to relieve the problem (iv) [15]. Peculiarities of the propagation of CRs [16] through the interstellar medium, e.g., a nonfactorizable rigidity and space dependence of the diffusion coefficient, have been considered as solutions for problem (ii).

In this work, we address the question if a single phenomenon can explain the entire set of features (i)–(vi). Perhaps the two most important clues how to solve these puzzles at one stroke are the problems (v) and (vi): the nearly scale invariance of hadronic interactions implies that the secondary fluxes produced in interactions of CRs on interstellar gas have a shape similar to the primary flux, if the grammage CRs cross is energy independent. Such an energy independence of the grammage is achieved if a young source contributes significantly to the observed local CR flux [17]. Moreover, the ratio $R(E) = F_{e^+}(E)/F_{\bar{p}}(E)$ of the positron and antiproton fluxes is then mainly predicted by the properties of hadronic interactions, being proportional to the ratio of their Z factors, $R = F_{e^+}/F_{\bar{p}} \propto Z_{e^+}/Z_{\bar{p}}$ [17,18]. As we showed in our previous Letter [17], the observed values of R lie within the range expected in this scenario. In contrast, for other primary sources of antimatter as dark matter annihilations or pulsars one expects naturally a much larger value of R. Recall also that the energy dependence $X \propto \mathcal{R}^{-\beta}$ with $\beta = 0.3$–0.5 expected in standard diffusion models would lead to a similar decrease of the secondary/proton ratios, which is not seen in Fig. 1. Finally, the observed plateau in the CR dipole anisotropy δ in the energy range 2–20 TeV can be also explained in the "local source" model, because the anisotropy δ of a single CR source is rigidity independent [19]. The decrease of the measured dipole anisotropy at lower energies, $E \lesssim 2$ TeV is naturally explained by an offset of the Earth with respect to magnetic field line going through the source [19]. Aim of the present work is to extend the papers [17,19] and to show that our scenario explains also naturally the remaining puzzles connected to the spectra of CR nuclei. Moreover, we have to ensure that the low-energy cutoff for the local CR flux does not spoil our successful explanation of the secondary fluxes obtained in Ref. [17].

Let us now sketch why a single CR source may give a dominant contribution to the local CR flux in the TV range. In the conventional diffusion approach, one uses a *smooth* distribution of CR sources and searches for a *stationary* solution of the coupled cascade equations. These two approximations seem natural in the GV–TV rigidity range if one adopts the isotropic diffusion of CRs with diffusion coefficient $D \simeq 10^{28}(\mathcal{R}/5\ \mathrm{GV})^{\beta}\ \mathrm{cm}^2/\mathrm{s}$ and $\beta \simeq 0.3$–0.5. If one, moreover, assumes that the CR sources are supernovae (SN) depositing some $\sim 10^{50}$ erg every $T \sim 30$ yr in the form of CRs which escape with the characteristic time scale $T_{\mathrm{esc}} \simeq \mathrm{few} \times 10^7\ \mathrm{yr}(\mathcal{R}/5\ \mathrm{GV})^{-\beta}$, then the flux from some 10^4 sources accumulates at low rigidities, forming a "sea" of Galactic CRs. As a result, Ref. [20] concluded that the dominance of a single source corresponds to a rare fluctuations and is therefore extremely unlikely in the isotropic diffusion picture.

The approximation of continuous injection might, however, not be valid if CRs propagate strongly anisotropically. Such an anisotropy may appear if the turbulent field at the considered scale does not dominate over the ordered component or if the turbulent field itself is anisotropic. As the authors of Ref. [21] stressed recently, anisotropic CR propagation is necessary, because otherwise CRs overproduce secondary nuclei like boron for any reasonable values of the strength of the turbulent field. As a result, they concluded that the number of sources contributing to the local CR flux is reduced by a factor $\mathcal{O}(100)$ relative to isotropic CR diffusion. For the special case of the Jansson-Farrar model [22] for the Galactic magnetic field, the authors of Refs. [23,24] obtained a satisfactory description of all data on Galactic primary CRs above $\simeq$200 GV, after the strength of the turbulent field was reduced. As a result of this reduction, CRs propagation becomes strongly anisotropic, and the diffusion coefficient perpendicular to the ordered field can be between 2 and 3 orders of magnitude smaller than the parallel one, $D_{\perp} \ll D_{||}$. Therefore, CRs spread perpendicular to the magnetic field line just $\sim$100 pc on the time scale of escape, compared to $\sim$1 kpc in the isotropic diffusion model. The smaller volume occupied by CRs from a single source leads to a smaller number of sources contributing substantially to the local flux, with only $\sim 10^2$ sources at $\mathcal{R} \sim 10$ GV and about $\sim$10 most recent SNe in the TV range.

Valuable information on recent local SNe comes from the discovery of radionuclides like ^{60}Fe in the deep ocean crust [25]. In particular, Ref. [26] derived the possible time sequence and locations of SN explosions from the mass spectrum of the perished members of certain nearby moving stellar groups. They found that 10–20 SNe are responsible for the formation of the Local Bubble, while the most recent ones happened 2–3 Myr ago and $\sim$100 pc away. According to Ref. [26], this SN, or a combined action of several SNe, may be responsible for the ^{60}Fe deposition on Earth.

In what follows, we show that the contribution to the flux of CR nuclei from a several Myr old supernova also explains the features (i) and (ii). Thus, the "local source" model provides a single explanation for the entire set of peculiar features (i)–(vi) in the GeV–TeV CR flux. We show that within such a model, measuring the parameters of the features (i)–(v) provides information on the most recent local SN. We also point out that the local source model is testable through its imprint on the boron-to-carbon (B/C) ratio. This ratio is predicted to reach a "plateau" in the energy range 1–10 TeV, where the local SN component provides the strongest contribution to the CR flux. The

level of the plateau is not a free parameter, but is fixed by the measurement of the positron flux at several hundred GeV. The (non)detection of this plateau in the B/C ratio could, therefore, be used to verify (falsify) the model. More generally, our model relies on the assumption that relatively few sources contribute to the CR flux. Therefore. the model predicts that the CR flux has several breaks which show up in secondary-to-primary ratios as B/C as steplike features.

II. COSMIC RAY PRIMARY NUCLEI

Measurements of the spectra of cosmic ray nuclei by PAMELA, CREAM, and AMS-02 have firmly established that the slopes of the spectra of individual nuclei are different: for instance, the helium spectrum above 10 GV becomes increasingly harder with increasing $\mathcal{R}$, compared to the proton spectrum. Moreover, the spectra of most of the nuclei show deviations from a single power law. One of the slope changes in these power laws is found in the $\mathcal{R} \sim$ 200–300 GV range where the proton spectrum $dN_p/d\mathcal{R} \propto \mathcal{R}^{-\gamma_p}$ hardens from $\gamma_p \simeq 2.8$–2.85 to $\gamma_p \simeq 2.6$–2.65. Another example is the helium spectrum $dN_{\rm He}/d\mathcal{R} \propto \mathcal{R}^{-\gamma_{\rm He}}$ which hardens from $\gamma_{\rm He} \simeq 2.78$ to $\gamma_{\rm He} \simeq 2.66$.

Both the difference and the changes in the slopes can be well described within the following simple model which includes two "template" functions, $F^{(1,2)}(\mathcal{R})$ for the shape of the spectra as a function of rigidity $\mathcal{R}$, summed with coefficients $C_A^{(1/2)}$ to fit the spectra of protons p and of nuclei with mass number A,

$$F_p(\mathcal{R}) = C_p^{(1)} F^{(1)}(\mathcal{R}) + C_p^{(2)} F^{(2)}(\mathcal{R}),$$
$$F_A(\mathcal{R}) = C_A^{(1)} F^{(1)}(\mathcal{R}) + C_A^{(2)} F^{(2)}(\mathcal{R}). \quad (1)$$

The low-energy component $F^{(1)}(\mathcal{R})$ represents the average CR flux in the local interstellar medium, as derived from γ-ray observations of nearby molecular clouds [27]. It is a broken power law $F^{(1)}(\mathcal{R}) \propto \mathcal{R}^{-\gamma_{1,2}}$ with the slope changing from $\gamma_1 = 2.4$ to $\gamma_2 = 3$ at the rigidity $\mathcal{R}_{\rm br} = 20$ GV. This form of the average spectrum is also consistent with the combined AMS-02, PAMELA, and Voyager 1 measurements of the local interstellar CR spectrum [28].

In addition to the average CR flux, we introduce the "local source" component $F^{(2)}(\mathcal{R})$, which is responsible for the deviations from the power-law extrapolation of the average flux component. We determine the shape of this component using two different approaches: A phenomenological one and a numerical method based on the calculation of CR trajectories in the Galactic magnetic field. In the phenomenological approach, we fix the shape of the local source component by fitting the combined AMS-02 and CREAM-III spectra of CR protons, as shown in Fig. 2. The resulting additional component of the spectrum is shown by the red solid line in Fig. 2. One can see that this component has a low-energy suppression.

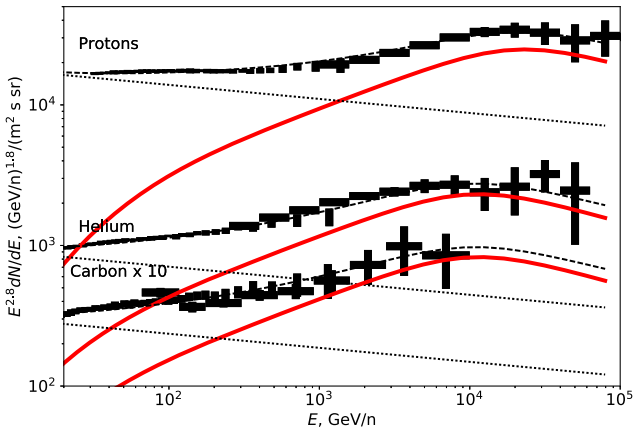

FIG. 2. The flux of CR protons and carbon measured by AMS-02 and CREAM-III as a function of energy/nucleon shown together with a two-component model consisting of the average CR spectrum (dotted lines) and the local source contribution (solid red lines).

This low-energy suppression is naturally explained within a numerical approach to the modeling of the CR flux from a local source. We calculate this flux using the method described in Ref. [17], see the Appendix for details. Motivated by the results of Ref. [26], we use as the distance to the supernova along the magnetic field line $d_{\parallel} = 100$ pc and an age 3 Myr. The Galactic magnetic field model adopted in the calculation is that of Ref. [22], where we rescaled the turbulent component by a factor $1/10$ as described in Refs. [23,24]. The maximal scale of the turbulent field modes was set to $L_{\rm max} = 25$ pc and a Kolmogorov power spectrum was used.

The resulting CR proton fluxes from a source with the distance $d_{\parallel} = 100$ pc along the magnetic field line and a varying perpendicular distance $d_{\perp}$ are shown in Fig. 3. Since the diffusion perpendicular to the magnetic field is

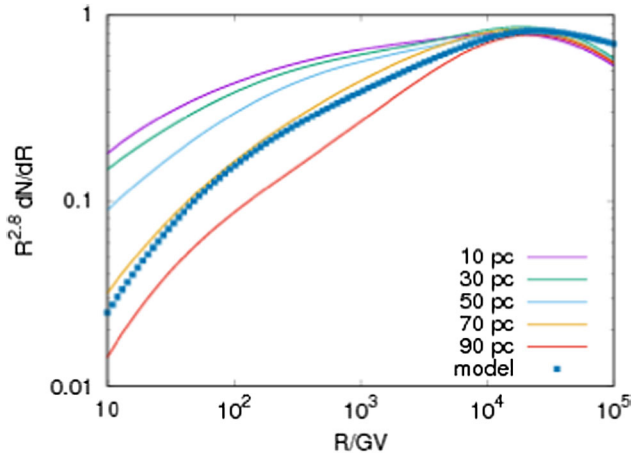

FIG. 3. CR rigidity spectrum for a source with $d_{\parallel} = 100$ pc and $d_{\perp} = 10$, 30, 50, 70 pc (from top to down) shown as lines compared to the proton spectrum in the phenomenological model shown by dots.

slow, a nonzero distance $d_\perp$ between the Solar System and the magnetic field line passing through the SN leads to a low-energy cutoff in the locally observed CR flux from this SN. Comparing to the proton flux in the phenomenological model shown by dots to those obtained in the trajectory approach, one sees that the model corresponds well to the case of $d_\perp \simeq 70$ pc.

The energy of the low-energy cutoff is constrained by the decrease of the dipole anisotropy of the CR flux below several hundred GeV [19]. The presence of a low-energy cutoff is also supported by the absence of an excess flux of secondary positrons in the energy range below ~30 GeV: a sizable contribution of protons from the local source in the energy range below several hundred GeV would produce an excess of $E < 30$ GeV positrons [17].

The propagation of CRs through the Galactic magnetic field is determined by the rigidity of the particles. Different nuclei with the same rigidity diffuse identically. This means that once the shape of the local source component is fixed from the fit to the proton spectrum, or based on our numerical results, the spectra of different nuclei are described by a set of fitting functions of the form (1), with the coefficients $C_A^{(i)}$ determined by the relative abundances of different nuclei in the average CR flux and in the local source components.

These relative abundances do not need to be identical for the two components. If one assumes that CRs are accelerated mostly at the forward shock of the expanding SN remnant, the coefficients $C_A^{(i)}$ are determined by the composition of the interstellar medium and the injection efficiencies of various elements. Since the local source exploded very likely in a star-forming region, deviations from the average values should be expected. Similarly, if a fraction of the CR flux originates from acceleration at the reverse shock, the coefficients $C_A^{(i)}$ also vary depending on the mass of the exploded star.

Figure 2 shows that the two component model based on the proton spectrum also provides a good fit to the helium spectrum over the entire energy range. The local source component of the helium spectrum, shown by the semi-transparent red curve is shifted by a factor of 2 in energy (per nucleon), compared to the local source component of the proton flux. Besides the relative normalization of the average and local source components for protons and helium are different. The same model is applicable to other nuclei, and the case of the CNO group is shown in Fig. 2 too. Finally, the change in the slope of the CR intensity from the local source visible at ≃10 TeV is connected to our choice of its maximal energy. Above this energy and up to the knee, the CR spectrum may be dominated by another, younger source.

III. POSITRONS AND ANTIPROTONS

In Ref. [17], we discussed already the contribution of a local source to the observed positron and antiproton flux. In that work we assumed, however, that the local source and the Solar System are connected by the same magnetic field line. In the present work, this assumption is relaxed and, therefore, the positron and antiproton fluxes need to be recalculated.

A. Propagation effects for the local flux

We have argued that the ratio of the secondary fluxes of positrons and antiprotons is determined by the properties of hadronic interactions, modulo propagation effect. As first step, let us look in more detail at the ratio $R = F_{e^+}(E)/F_{\bar{p}}(E)$ of the positron and antiproton flux. Neglecting propagation effects, R is given by the ratio of the Z factors of positron and antiprotons, respectively. The latter are defined for the secondary type j via its inclusive spectrum $d\sigma_j(E, z_j)/dz_j$, $z_j = E_j/E$, as

$$Z_j(E_j, \alpha) = \frac{1}{\sigma_{\rm inel}} \int_0^1 dz z^{\alpha-1} \frac{d\sigma_j(E_j/z, z)}{dz}, \qquad (2)$$

if the primary protons follow the power law $dN/dE \propto E^{-\alpha}$. In Ref. [18], this ratio was calculated analytically in the asymptotic limit, i.e., for energies well above the threshold $E \gg E_{\rm th}$, as $R = 1.8 \pm 0.5$ for a power-law spectrum of protons with slope $\alpha = 2.8$. We use the modified version QGSJET-IIm [29] presented in Ref. [30] to calculate the positron and antiproton secondary fluxes. For the same setup, a power law with $E_{\rm max} \gg E$, we obtain $R = 1.8$ ($\alpha = 2.6$) and $R = 1.6$ ($\alpha = 2.8$). Using the spectrum given by Eq. (1) with $E_{\rm max} = 1$ PeV as a high-energy cutoff, we find that the asymptotic limit represents only in a small energy range a good approximation: below secondary energies $E \simeq 100$ GeV, the threshold suppression of antiproton production increases R, while the soft positron spectra in forward direction lead towards $E_{\rm max}$ to a decrease of R.

Let us now discuss how propagation effects modify the secondary/proton ratio. Positrons and antiprotons have lower energies than their parent cosmic rays and spread therefore more slowly into the interstellar medium. As a result, they occupy a smaller volume than their parent cosmic rays. Within this smaller volume, the positron and antiproton fluxes are enhanced compared to the reference flux which one would obtain assuming that secondaries propagate in the same way as the primary particles. In contrast, at larger perpendicular distances, the secondary flux is suppressed relative to the reference flux, because the secondaries diffuse slower.

In Ref. [17], we calculated analytically a correction factor for the positron and antiproton flux for the particular case, when the observer is situated at the same magnetic field line as the source. In this case, the positron and the antiproton flux experience an enhancement by a factor of about 2. Figure 4 shows the result of our numerical calculations corresponding to the more generic situation

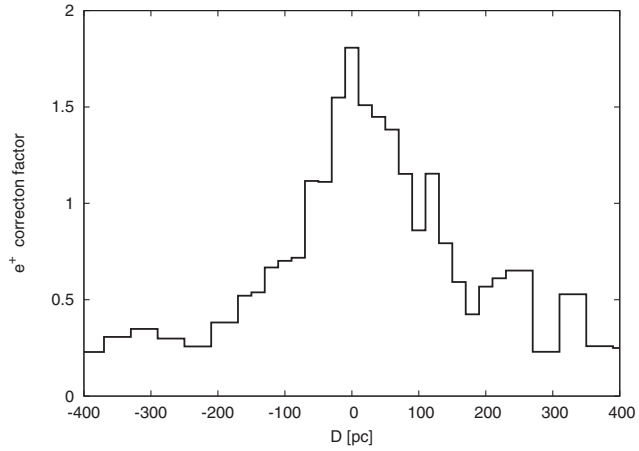

FIG. 4. Correction factor for positrons with energy 100 GeV as function of the perpendicular distance $d_\perp$ to the magnetic field line.

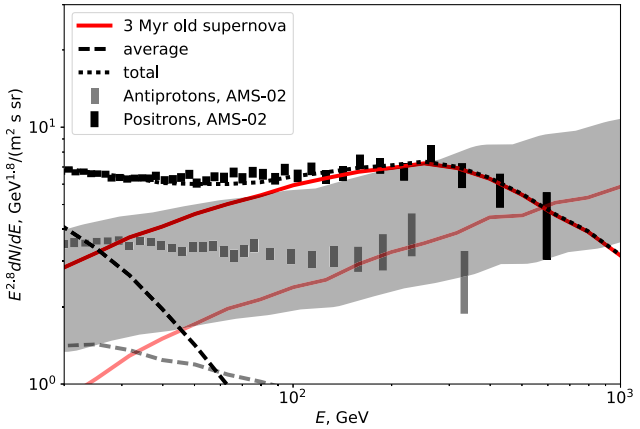

FIG. 5. Positron and antiproton fluxes measured by AMS-02 compared to the contributions for the local source (red/rose solid curves) and average (dashed black/gray) components. Wide gray band shows the ±50% uncertainty band for the sum of the antiproton fluxes of the two components.

when the observer is separated by the distance $d_\perp$ from the magnetic field line going through the source. Here, the positive and negative values of $d_\perp$ correspond to the case that the observer is displaced towards the Galactic center or away, respectively.

This correction factor is calculated in following way. We divide the production time in six intervals of 0.5 Myr duration. In each time interval, we assume that positrons are produced by protons with 20 times higher energy, which are spatially distributed according to their numerically calculated trajectories. Once produced, we propagate the positrons the remaining time up to 3 Myr. Then, we obtain the positron fluxes at various perpendicular distances summing up the partial fluxes from all time intervals. Dividing finally these fluxes by the proton flux (at the same energy), we obtain the correction factor due to the difference in the propagation between protons and positrons. From Fig. 4, one sees that for $d_\perp = 0$ the correction factor is close to 2, as calculated analytically in Ref. [17]. Increasing $d_\perp$, the correction factor decreases, falling below 1 at $d_\perp \sim 100$ pc.

B. Secondary fluxes

We now turn to the resulting flux of positrons and antiprotons produced by CRs with the spectra $F^{(1)}(\mathcal{R})$ and $F^{(2)}(\mathcal{R})$. We obtain a reasonable fit of the measured positron flux for a range of perpendicular distances, $d_\perp \sim \pm(50-90)$ pc. In Fig. 5, we show the positron flux for the case $d_\perp = 70$ pc, assuming that the CRs from the local source have traversed the column density of matter $X = 1.2$ g/cm^2, while we use $X = 11.4(\mathcal{R}/10\ \mathrm{GV})^{-1/3}$ g/cm^2 for the average flux of "sea" CRs. Our estimate for the grammage crossed by CRs emitted from the local source based on the positron flux suffers from uncertainties in the distance between the magnetic field lines of the source and of the observer. We use the reference distance 70 pc at which the correction factor for the positron flux at 100 GeV is about 1. Taking the distance range ±20 pc would change the correction factor by ≃50%, as it is clear from Fig. 4. This uncertainty propagates to a 50% uncertainty in the grammage. We take this uncertainty into account in the analysis reported below. Note, however, that additional uncertainties in the Galactic magnetic field model and the value of $d_\perp$ exist. As it was previously shown in Ref. [17], the local source contribution explains the excess flux of CR positrons. The flux of antiprotons agrees within errors with that measured by AMS-02 up to 300 GeV. The grammage $X = (1.0\text{–}1.4)$ g/cm^2 for CRs from the local source is larger than the one found in Ref. [17], both because of the used larger age of the source and the smaller proton flux caused by the nonzero offset of the source. It is a factor ≃2 larger than expected for CRs propagating in a gas density following a Nakanishi-Sofue profile [31]. Taking into account possible local deviations from the global gas profile as well as astrophysical uncertainties, we consider this as a minor deviation.

Recently, the measurements of the positron spectrum did not extend to a high enough energy to probe the effect of Compton cooling on the positrons injected by the local source. Meanwhile, an updated measurement of the positron spectrum by AMS-02 has appeared [32]. This measurement reveals a break in the positron spectrum at 300 GeV. Such a break is expected in the local source model [17], because positrons with energies around 300 GeV loose energy via synchrotron and inverse Compton emission on the time scale of 2–3 Myr. Thus, the spectrum of positrons from the local source is expected to have a cooling break at about 300 GeV [17], with the slope changing by $\Delta\alpha = 1$, as shown in Fig. 5. The presence of the cooling break is consistent with the updated

AMS-02 measurement, shown by the black data points in the same figure. The measurement of the break energy determines the time elapsed since the injection of CRs by the supernova.

Contrary to positrons, antiprotons do not suffer from Compton cooling, and thus, no cooling break is expected in the antiproton spectrum. The extension of the AMS-02 measurements to energies above 300 GeV should reveal a nearly power-law continuation of the antiproton flux.

IV. ELECTRONS

We discuss now the electron fluxes expected in our model. Similar to CR nuclei, electrons are injected as primaries in the acceleration process. Neglecting energy losses, the contribution for the electron spectrum from the local source has therefore the same functional form as the proton spectrum and can be expressed as $C_{e^-}^{(2)} F^{(2)}(\mathcal{R})$. The normalization constant $C_{e^-}^{(2)}$ is related to the only poorly restricted electron/proton ratio $K_{\rm ep}$ at injection which we choose as $K_{\rm ep} = 4 \times 10^{-3}$. The energy losses via synchrotron and inverse Compton emission lead to an exponential cutoff for primary electrons, since they are all injected instantaneously 2.7 Myr ago. From the data in the positron spectrum, we choose the break at $E_{\rm br} = 300$ GeV. The spectrum of primary electrons from the local source is therefore modified as

$$C_{e^-}^{(2)} F^{(2)}(\mathcal{R}) \to C_{e^-}^{(2)} F^{(2)}(\mathcal{R}) \exp(-E/E_{\rm br}).$$

The low-energy component $F^{(1)}(\mathcal{R})$ representing the average CR flux from sources in the disk is modified by energy losses as $F^{(1)}(\mathcal{R}) \to F^{(1)}(\mathcal{R})(E/E_0)^{0.5}$ [33]. In Fig. 6, we compare the resulting electron intensity compared to the data from AMS-02. In addition, we also show the flux of secondary electrons which are continuously produced by proton-gas interactions. This flux coincides with the secondary flux of positrons from the local source discussed earlier and becomes dominant above 500 GeV.

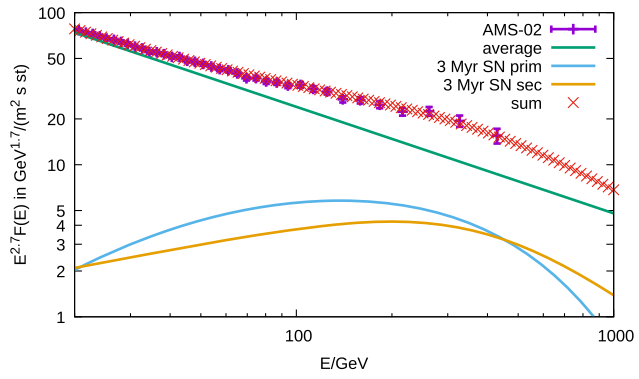

FIG. 6. Electron fluxes measured by AMS-02 compared to the contributions for the local source (red/rose solid curves) and average (dashed black/gray) components.

V. COSMIC RAY SECONDARY NUCLEI AND THE B/C RATIO

Apart from positrons and antiprotons, the propagation of CRs injected by the local source results in the production of secondary cosmic ray nuclei. In particular, the spallation of primary carbon and oxygen generates a secondary boron flux. Similar to the flux of electrons and positrons, the flux of boron nuclei is expected to have two contributions: one generated by the average cosmic ray flux and the second one produced by the carbon injected by the local recent supernova.

Contrary to the positron and antiproton fluxes, the local source contribution to the boron flux is expected to appear around TV, rather than 100 GV. This is because the typical rigidity of positrons and antiprotons produced in CR interactions is below 10% of the rigidity of the primary cosmic ray, while the rigidity of boron nuclei produced in spallation of the carbon nuclei is identical or very similar to that of the primary carbon.

We adopt a simple leaky-box model approach,

$$\frac{F_B}{F_C} \simeq (X/20\ \mathrm{g/cm^2})/(1 + X/(13\ \mathrm{g/cm^2})) \qquad (3)$$

using as parameters those determined in Refs. [34,35]: The characteristic column densities 20 g/cm^2 and 13 g/cm^2 correspond to the grammage on which a significant part of the carbon is transformed into boron and a significant part of boron is destroyed by spallation, respectively. Within the considered model the total carbon flux is $F_C = F_C^{(1)} + F_C^{(2)}$.

In both isotropic and anisotropic diffusion models, the residence time of CRs in the interstellar medium scales as a power law of particle rigidity $T \propto \mathcal{R}^{-\beta}$ in the energy range of interest. The column density traversed by the CRs belonging to the average flux component scales as $X^{(1)} = n_{\rm ISM} T \propto \mathcal{R}^{-\beta}$ so that the expected rigidity dependence of the B/C ratio is a power law, $F_B/F_C \propto \mathcal{R}^{-\beta}$ for $F_B/F_C \ll 0.7$. At the same time, carbon injected by the local source has traversed the fixed column density $\simeq (1.0 - 1.4)$ g/cm^2 since the moment of injection, which is determined by our fit to the positron spectrum in the previous section. The overall amount of boron contained in the CR flux is, therefore,

$$\frac{F_B}{F_C} = \frac{X^{(1)}/(20\ \mathrm{g/cm^2})}{(1 + X^{(1)}/(13\ \mathrm{g/cm^2}))} \frac{F_C^{(1)}}{F_C} + \frac{X^{(2)}/(20\ \mathrm{g/cm^2})}{(1 + X^{(2)}/(13\ \mathrm{g/cm^2}))} \frac{F_C^{(2)}}{F_C}. \qquad (4)$$

This flux ratio is shown in Fig. 7 together with the measurements from AMS-02 [36]. The thin dashed black and gray lines show the rigidity scaling of the B/C ratio which would be found in the absence of the local source component. We have assumed the power-law slope $\beta = 1/3$

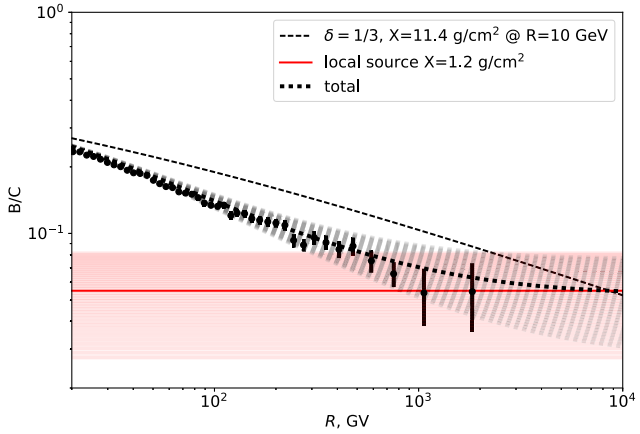

FIG. 7. Rigidity dependence of a B/C ratio of the average cosmic ray flux in a model with a diffusion coefficient determined by the Kolmogorov turbulence spectrum of a magnetic field (thin dashed line), by a fixed grammage traversed by the carbon nuclei originating from a several Myr old local supernova (red solid line and shaded uncertainty band) and in a model in which the observed cosmic ray flux is a sum of average and local source contributions in proportions deduced from the template fit to the carbon spectrum (black dotted line and gray uncertainty band).

for the rigidity dependence of the grammage, appropriate for Kolmogorov turbulence. Note that the slope of the B/C ratio disagrees at low rigidities with the measurements. The red and rose horizontal lines correspond to the B/C ratio which would be found if the observed flux would be fully provided by the local source for the grammage 1.2 ± 0.6 g/cm^2 (the 50% uncertainty range takes into account the uncertainty of the estimate based on positron flux from the local source). The thick dotted black and gray lines correspond to the case of the two-component carbon flux shown in Fig. 2. Above few $\times 100$ GV, the B/C ratio flattens and reaches finally a plateau corresponding to the B/C ratio produced by the local source.

The plateau in the B/C ratio and an approximately constant antiproton-proton ratio predicted in the local source model distinguish this model from the "reacceleration model" which, according to Refs. [37,38], predicts rising antiproton-proton and B/C ratios.

In our analysis, we have considered a model with a single local source superimposed onto a smooth "sea" of CRs. In reality, the transition between the rigidity range where the assumption of continuous CR is justified and discrete sources is gradual. This should be reflected in the rigidity dependence of the B/C ratio: several plateaulike features might be present, so that the overall plot should have a set of "steps" corresponding to plateaus connected to several recent injection episodes.

VI. DETECTABILITY OF THE LOCAL SOURCE SIGNATURE IN THE B/C RATIO

Steplike features in the energy dependence of the B/C ratio and, in particular, a plateau $\mathrm{B/C} \sim \text{few} \times 0.01$ above TV are specific predictions of the local source model. The detection of such a plateau or other steplike features would provide a powerful test of the model. This test would be complementary to the test of another prediction of the model: a simple power-law extension of the antiproton flux into the TeV band from lower energies, i.e., no softening of the spectrum, cf. with Fig. 5. The theoretical predictions for the antiproton flux suffer from uncertainties in the production cross section, of the average primary CR spectrum, and of the propagation of CRs through the interstellar medium and magnetic fields. In contrast, the theoretical predictions for the B/C ratio expected from the average CR flux are not sensitive to the details of the CR spectra in the interstellar medium. They are largely determined by the energy dependent grammage traversed by the carbon and oxygen nuclei during their residence time in the interstellar medium.

The energy range of the measurement of the B/C ratio by AMS-02 (shown in Fig. 7) only touches the predicted "plateau" energy range. AMS-02 measurements are intrinsically restricted to the rigidity range below 10 TV because of the limited charge resolution at higher rigidities. Dedicated detectors optimized for the measurement of elemental composition of the CR flux in the multi-TV range are needed for the detection of the local source related plateau of the B/C ratio.

Measurements by the CREAM balloon born detector also do not extend to the rigidity range of interest. The carbon nuclei flux is at the level of $F_C = 1.5^{+1.0}_{-0.6} \times 10^{-9}$ $1/(\mathrm{m}^2\ \mathrm{sr\,s\,GeV/n})$ at the energy per nucleon $E/A = 7.4$ TeV (corresponding to the rigidity $\mathcal{R} = cp/Z \simeq 15$ TV). A CREAM-type detector accumulates the carbon signal at the rate of 0.2 events per day at this energy/rigidity. Only five carbon nuclei were detected in the first CREAM flight in this energy range. No boron nuclei are detectable in a flight campaign if the B/C ratio is at the expected plateau level, $F_B \sim 0.06 F_C$.

Larger event statistics could potentially be accumulated in the case of a multiyear exposure with a space-based detector, like ISS-CREAM or NUCLEON. A nominal five-year CREAM-like space detector could yield the event statistics of about 215 events in the energy range of interest. The expected statistics of the boron cosmic rays is about 12 events accumulated over the mission time span. This shows that measurement of the flattening of the energy dependence of the B/C ratio would be challenging with planned or operating space-based CR detectors. Larger detectors and/or longer exposure times are desirable for the detection of the predicted plateau.

Another prediction of our model are steplike features in the B/C ratio: the "average" flux is the sum of $N \simeq 10$–20 local SNe, each of it producing its own plateau. Summing up these contributions will produce a steplike feature in the B/C ratio, with the plotted $1/3$ power law emerging only in the $N \to \infty$ limit. These features might be present at lower

energies and would be more readily detectable increasing the statistics of the B/C signal.

VII. DISCUSSION AND CONCLUSIONS

We have shown that the whole set of known peculiar features (i)–(vi) of the locally observed CR spectrum can be explained within a single self-consistent model. This model takes into account the contribution to the CR flux of a supernova which has injected CRs within a distance of about 100 pc from the Sun some 2–3 Myr ago. It is likely that this supernova is connected to the deposition of ^{60}Fe isotopes in the deep ocean crust of the Earth.

In Ref. [19], we showed that a CR source with age $T = 2$ Myr and distance $d = 200$ pc leads to a dipole anisotropy $\delta \simeq 5 \times 10^{-4}$, assuming quasi-Gaussian propagation of CRs. This value corresponds to the central value of the observed range for δ. For the source distance and age used in the present work, the dipole anisotropy $\delta \simeq 2 \times 10^{-4}$ follows, which corresponds to the values at the lower edge of the error band shown in Fig. 2 of Ref. [19]. As a possible reason for this small deviation, we note that the local source may reside inside the complex of the local and loop 1 superbubble. As a result, the bubble wall between loop 1 and the local superbubble might act as an "effective" CR source, leading to deviations from the naive dipole formula.

Figure 2 shows the explanation for the features (i) and (ii). The difference in the spectral slopes of different nuclear species in the CR flux is explained by the slightly different normalization of the local source contribution to the flux of different nuclei (related to the particular chemical composition of the SN environment) and due to the rigidity dependent shifts of the local source component along the energy axis. The breaks in the spectra of individual nuclei at several hundred GeV are due to the fact that the local source component gradually starts to dominate over the average cosmic ray flux component at higher energies.

The measurement of the cooling break in the spectrum of CR positrons at 300 GeV (cf. with Fig. 5) determines the time elapsed since the episode of CR injection by the supernova. This time is consistent with the age of the supernova deduced from the measurements of the ^{60}Fe deposition in the deep ocean crust. The presence of the positrons and antiprotons produced in interactions of the CRs injected by the supernova explains the features (iii)–(iv).

Low energy cosmic rays from the supernova have not yet reached the ordered magnetic field line passing through the Solar System. The low-energy suppression of the local source component explains the energy dependence of the dipole anisotropy (vi). This suppression is also evident from the phenomenological fit of the shape of the local source contribution as an excess flux over the average flux of CRs in the local Galaxy, as deduced from the γ-ray observations of nearby molecular clouds.

The model discussed above is overconstrained which allows one to falsify it. Four testable predictions of the model are the persistence of a nearly constant slope of the antiproton spectrum in the energy range beyond 300 GeV, the positron-electron ratio R, steplike features, and the flattening of the boron-to-carbon ratio to a "plateau" level of $F_B/F_C \sim 0.06$ in the 1–10 TV range. These tests are complementary. The test based on the antiproton-proton and the positron-antiproton ratio suffers from uncertainties in theoretical calculation of propagation of secondary particles through Galactic magnetic field, as illustrated in Sec. III. The tests based on the measurement of the B/C ratio are challenging from the experimental point of view. The detection of the plateau requires a decade-scale exposure with space-based cosmic ray detectors like ISS-CREAM and NUCLEON. While the exact numerical values of these predictions is influenced in particular by the modeling of the local magnetic structure and the position of the local source, the presence of these features depends only on the dominance of a local source in the CR flux in the ~1–30 TeV range.

We also note that a supernova as close as 100 pc may also impact the Earth's atmosphere and biota, and the absence of a major extinction 2–3 Myr ago is another evidence for the low-energy suppression of the CR flux from the local source [39].

Finally, we want to stress the differences between our scenario and related models. In Ref. [40], the effect of one or several nearby SN explosions on the secondary ratios was considered. Since these authors assumed a standard isotropic diffusion, both the primary and the secondary fluxes of these sources in general do not dominate the measured fluxes today. In particular, the scenario of Ref. [40] therefore can not explain the plateau in the dipole anisotropy or the breaks in the primary spectra. In order to enhance the secondary fluxes, the SN explosions had to occur in a dense environment, as, e.g., a molecular cloud. The authors of Ref. [38] also assumed standard isotropic diffusion and split the contribution of all SNRs into a young and an old component. Their main prediction is a featureless B/C ratio, in contrast to the steplike features typical for our model.

ACKNOWLEDGMENTS

This research was supported in part with computational resources at NTNU provided by NOTUR, http://www.sigma2.no. We would like to thank the anonymous referee for valuable comments which helped to improve our manuscript.

APPENDIX: CALCULATION OF TRAJECTORIES

In the standard approach to cosmic ray (CR) propagation, the time evolution in phase space is approximated as a diffusion process. Including CR interactions in the resulting

transport equation allows one to calculate self-consistently fluxes of primary and secondary CRs. However, this approach has several disadvantages: most importantly, the diffusion approximation breaks down in several regimes [23,41,42]. Moreover, the diffusion tensor is an external input which can be only loosely connected to fundamental properties of the Galactic magnetic field (GMF). Therefore, we calculate the path of individual CRs solving the equations of motion of particles propagating in the GMF. In particular, we employ the code described and tested in Ref. [43], which uses nested grids. Our procedure to use such grids is the following: for the largest scale, we choose $L_{\max} = 25$ pc according to the recent LOFAR measurement of the maximal scale of magnetic field fluctuations in the disk [44]. Then, we use up to four nested grids, which cover five decades in scale such that the smallest resolved length scale is a factor of 10 below the resonance scale for a CR with 10 TV rigidity. This corresponds to the lowest rigidity for which we made direct calculations in Ref. [17].

For the calculation of the local CR flux, we have divided the nearby Galaxy in cells and saved the length of CR trajectories per cell. Compared to Ref. [17], we increased the number of cells and observers: we divided the Galactic plane into a nonuniform grid with a cell size 20 pc × 20 pc at the position of the SN, which gradually increases to 100 pc × 100 pc at distances more than 500 pc. The vertical height of these cells was chosen as 20 pc. This allowed us to calculate simultaneously the flux at various places with a differing perpendicular distance to the regular magnetic field line which goes through the SN (see Fig. 3).

Several detailed models for the regular component of the GMF exist, and two of the most recent and detailed ones are the models of Jansson-Farrar [22] and of Pshirkov *et al.* [45]. Reference [46] compared both models and found that they lead qualitatively to the same predictions for CR propagation. The turbulent part of the magnetic field can be characterized by the power spectrum $\mathcal{P}(\boldsymbol{k})$ and the correlation L_c of its fluctuations. Assuming a power law $\mathcal{P}(k) \propto k^{-\alpha}$ for the spectrum, the maximal length $L_{\max}$ of the fluctuations and the correlation length L_c are connected by $l_c = (\alpha - 1)L_{\max}/(2\alpha)$. An important constraint on CR propagation models comes from ratios of stable primaries and secondaries produced by CR interactions on gas in the Galactic disk. Employing the Jansson-Farrar model, Ref. [43] found that the B/C ratio can be reproduced by choosing as the maximal length of the fluctuations $L_{\max} = 25$ pc and $\alpha = 5/3$, if the turbulent field is rescaled to one tenth of the value proposed by Jansson-Farrar [22]. For this choice of parameters, CR propagation in the Jansson-Farrar model reproduces a large set of local CR measurements, and we used these parameters in this work. In particular, the B/C ratio measured by AMS-02 [36] can be nicely reproduced using a Kolmogoroff power spectrum, $\alpha = 5/3$, as we have shown here.

Cosmic rays with energies $E \lesssim 100$ TeV propagate in the diffusive regime, using our standard magnetic field model. In the energy range 10–100 TeV, we showed that the diffusion is self-similar, i.e., the propagation at $E < E_0$ follows the relation $t' = t(E_0/E)^{1/3}$, see Fig. 4 in Ref. [17]. Here, we applied this self-similar solution to all energies lower than $E_0 = 10^{14}$ eV.

[1] A. W. Strong, I. V. Moskalenko, and V. S. Ptuskin, Annu. Rev. Nucl. Part. Sci. **57**, 285 (2007); C. Evoli, D. Gaggero, D. Grasso, and L. Maccione, J. Cosmol. Astropart. Phys. 10 (2008) 018.

[2] O. Adriani *et al.* (PAMELA Collaboration), Science **332**, 69 (2011).

[3] M. Aguilar *et al.* (AMS Collaboration), Phys. Rev. Lett. **114**, 171103 (2015).

[4] M. Aguilar *et al.* (AMS Collaboration), Phys. Rev. Lett. **115**, 211101 (2015).

[5] Y. S. Yoon *et al.*, Astrophys. J. **728**, 122 (2011).

[6] H. S. Ahn *et al.*, Astrophys. J. **707**, 593 (2009).

[7] Y. S. Yoon *et al.*, Astrophys. J. **839**, 5 (2017).

[8] O. Adriani *et al.* (PAMELA Collaboration), Nature (London) **458**, 607 (2009); O. Adriani *et al.*, Phys. Rev. Lett. **111**, 081102 (2013).

[9] L. Accardo *et al.* (AMS Collaboration), Phys. Rev. Lett. **113**, 121101 (2014); M. Aguilar *et al.* (AMS Collaboration), Phys. Rev. Lett. **113**, 121102 (2014).

[10] O. Adriani *et al.* (PAMELA Collaboration), Phys. Rev. Lett. **105**, 121101 (2010).

[11] M. Aguilar *et al.* (AMS Collaboration), Phys. Rev. Lett. **117**, 091103 (2016).

[12] G. Di Sciascio and R. Iuppa, arXiv:1407.2144.

[13] A. K. Harding and R. Ramaty, Proc. 20th ICRC, Moscow, **2**, 92 (1987); A. Boulares, Astrophys. J. **342**, 807 (1989); F. A. Aharonian, A. M. Atoyan, and H. J. Völk, Astron. Astrophys. **294**, L41 (1995).

[14] For a review, see M. Cirelli, *Proc. Sci.*, ICRC2015 (2016) 014.

[15] G. Giesen, M. Boudaud, Y. Gnolini, V. Poulin, M. Cirelli, P. Salati, and P. D. Serpico, J. Cosmol. Astropart. Phys. 09 (2015) 023; C. Evoli, D. Gaggero, and D. Grasso, J. Cosmol. Astropart. Phys. 12 (2015) 039; M. J. Boschini *et al.*, Astrophys. J. **840**, 115 (2017).

[16] N. Tomassetti, Astrophys. J. **752**, L13 (2012).

[17] M. Kachelriess, A. Neronov, and D. V. Semikoz, Phys. Rev. Lett. **115**, 181103 (2015).

[18] P. Lipari, Phys. Rev. D **95**, 063009 (2017).
[19] V. Savchenko, M. Kachelriess, and D. V. Semikoz, Astrophys. J. **809**, L23 (2015).
[20] Y. Genolini, P. Salati, P. Serpico, and R. Taillet, Astron. Astrophys. **600**, A68 (2017).
[21] G. Giacinti, M. Kachelriess, and D. V. Semikoz, arXiv:1710.08205.
[22] R. Jansson and G. R. Farrar, Astrophys. J. **757**, 14 (2012); **761**, L11 (2012).
[23] G. Giacinti, M. Kachelriess, and D. V. Semikoz, Phys. Rev. D **90**, R041302 (2014).
[24] G. Giacinti, M. Kachelriess, and D. V. Semikoz, Phys. Rev. D **91**, 083009 (2015).
[25] K. Knie, G. Korschinek, T. Faestermann, C. Wallner, J. Scholten, and W. Hillebrandt, Phys. Rev. Lett. **83**, 18 (1999); N. Benitez, J. Maiz-Apellaniz, and M. Canelles, Phys. Rev. Lett. **88**, 081101 (2002); A. Wallner *et al.*, Nature (London) **532**, 69 (2016); L. Fimiani *et al.*, Phys. Rev. Lett. **116**, 151104 (2016).
[26] M. M. Schulreich, D. Breitschwerdt, J. Feige, and C. Dettbarn, Astron. Astrophys. **604**, A81 (2017).
[27] A. Neronov, D. V. Semikoz, and A. M. Taylor, Phys. Rev. Lett. **108**, 051105 (2012); A. Neronov, D. Malyshev, and D. V. Semikoz, Astron. Astrophys. **606**, A22 (2017).
[28] A. C. Cummings, E. C. Stone, B. C. Heikkila, N. Lal, W. R. Webber, G. Jóhannesson, I. V. Moskalenko, E. Orlando, and T. A. Porter, Astrophys. J. **831**, 18C (2016).
[29] S. Ostapchenko, Phys. Rev. D **77**, 034009 (2008); **83**, 014018 (2011).
[30] M. Kachelriess, I. V. Moskalenko, and S. S. Ostapchenko, Astrophys. J. **803**, 54 (2015).
[31] H. Nakanishi and Y. Sofue, Publ. Astron. Soc. Jpn. **55**, 191 (2003); Publ. Astron. Soc. Jpn. **58**, 847 (2006).
[32] S. Ting, colloquium at CERN, 16.12.2016, https://indico.cern.ch/event/592392/.
[33] A. D. Panov, J. Phys. Conf. Ser. **409**, 012004 (2013).
[34] W. R. Webber, F. B. McDonald, and A. Lukasiak, Astrophys. J. **599**, 582 (2003).
[35] K. Blum, B. Katz, and E. Waxman, Phys. Rev. Lett. **111**, 211101 (2013).
[36] M. Aguilar *et al.* (AMS Collaboration), Phys. Rev. Lett. **117**, 231102 (2016).
[37] P. Blasi, Phys. Rev. Lett. **103**, 051104 (2009); P. Blasi and P. D. Serpico, Phys. Rev. Lett. **103**, 081103 (2009); P. Mertsch and S. Sarkar, Phys. Rev. Lett. **103**, 081104 (2009); For a different view, see also M. Kachelriess, S. Ostapchenko, and R. Tomas, Astrophys. J. **733**, 119 (2011); M. Kachelriess and S. Ostapchenko, Phys. Rev. D **87**, 047301 (2013).
[38] N. Tomassetti and F. Donato, Astrophys. J. **803**, L15 (2015).
[39] B. C. Thomas, E. E. Engler, M. Kachelriess, A. L. Melott, A. C. Overholt, and D. V. Semikoz, Astrophys. J. **826**, L3 (2016); A. L. Melott, B. C. Thomas, M. Kachelriess, D. V. Semikoz, and A. C. Overholt, Astrophys. J. **840**, 105 (2017).
[40] Y. Fujita, K. Kohri, R. Yamazaki, and K. Ioka, Phys. Rev. D **80**, 063003 (2009).
[41] G. Giacinti, M. Kachelriess, and D. V. Semikoz, Phys. Rev. Lett. **108**, 261101 (2012).
[42] G. Giacinti, M. Kachelriess, and D. V. Semikoz, Phys. Rev. D **88**, 023010 (2013).
[43] G. Giacinti, M. Kachelriess, D. V. Semikoz, and G. Sigl, J. Cosmol. Astropart. Phys. 07 (**2012**) 031.
[44] M. Iacobelli *et al.*, Astron. Astrophys. **558**, A72 (2013).
[45] M. S. Pshirkov, P. G. Tinyakov, P. P. Kronberg, and K. J. Newton-McGee, Astrophys. J. **738**, 192 (2011); M. S. Pshirkov, P. G. Tinyakov, and F. R. Urban, Mon. Not. R. Astron. Soc. **436**, 2326 (2013).
[46] G. Giacinti, M. Kachelriess, and D. V. Semikoz, Phys. Rev. D **91**, 083009 (2015).